J|A|C|S
ARTICLES
Published on Web 08/17/2006

Large Molecular Assembly of Amphotericin B Formed in Ergosterol-Containing Membrane Evidenced by Solid-State NMR of Intramolecular Bridged Derivative

Nobuaki Matsumori,* Yuri Sawada, and Michio Murata*

Contribution from the Department of Chemistry, Graduate School of Science, Osaka University, Toyonaka, Osaka 560-0043, Japan

Received May 17, 2006; E-mail: murata@ch.wani.osaka-u.ac.jp; matumori@ch.wani.osaka-u.ac.jp

Abstract: Amphotericin B (AmB **1**) is known to assemble and form an ion channel across biomembranes. We have recently reported that conformation-restricted derivatives of AmB **2**−**4** show different ergosterol preferences in ion-channel assays, which suggested that the orientation of the mycosamine strongly affects the sterol selectivity of AmB. The data allowed us to assume that compound **3** showing the highest selectivity would reflect the active conformation of AmB in the channel assembly. In this study, to gain further insight into the active conformation of AmB, we prepared a new intramolecular-bridged derivative **5**, where the linker encompassed a hydrophilic glycine moiety. The derivative has almost equivalent ion-channel activity to those of AmB and **3**. The antifungal activity of **5** compared with **3** improves significantly, possibly because the increasing hydrophilicity in the linker enhances the penetrability through the fungal cell wall. Conformation of **5** was well converged and very similar to that of **3**, thus further supporting the notion that the conformations of these derivatives reproduce the active structure of AmB in the channel complex. Then we used the derivative to probe the mobility of AmB in the membrane by solid-state NMR. To measure dipolar couplings and chemical shift anisotropies, we incorporated [1-^{13}C,^{15}N]glycine into the linker. The results indicate that **5** is mostly immobilized in ergosterol-containing DMPC bilayers, implying formation of large aggregates of **5**. Meanwhile some fraction of **5** remains mobile in sterol-free DMPC bilayers, suggesting promotion of AmB aggregation by ergosterol.

Introduction

For over 40 years, amphotericin B (AmB, **1**) has been a standard drug for treatment of deep-seated systemic fungal infections.[1−3] Due to lack of better alternatives as well as the scarce occurrence of resistant strains,[4] the clinical importance of AmB has been unchanged. It is now widely accepted that AmB in a phospholipid membrane associates with sterols to form barrel-stave type pores, with their polyhydroxy side pointing inward and their lipophilic heptaene part directing outward.[5,6] The occurrences of such molecular assemblies in a fungal cell membrane increases ion permeability and alters membrane potentials, ultimately leading to the cell death.[6−9] The pharmacological action of AmB is based on its selective toxicity against eukaryotic microbes over mammalians. It has been repeatedly shown that ergosterol-containing fungal membranes are more sensitive to AmB than cholesterol-containing mammalian membranes (Chart 1).[8,10,11]

The structure of AmB comprises two rigid fragments, a macrolide ring and a mycosamine sugar moiety, which are linked by a rotatable β-glycosidic bond. Their relative position is thought to control AmB−AmB and AmB−sterol interactions, where inter- and intramolecular hydrogen bonds play crucial roles.[12,13] To reveal the relationship between the orientation of aminosugar and activities, we have recently prepared intramolecular bridged derivatives of AmB **2**−**4** (Chart 2), where carboxyl and amino groups are bridged with different lengths of alkyl chains.[14] Consequently, **2**−**4** showed different ergosterol preferences in membrane-permeabilizing activity, probably due to the alteration of the amino-sugar orientation induced by the alkyl bridge. In particular, the ergosterol selectivity of **3**, of which amino-sugar orientation is immobilozed by the bridge, markedly exceeds that of AmB. These results allowed us to assume the conformation of **3** somewhat reflects the active structure of AmB in the channel complex. The bridged deriva-

(1) Gallis, H. A.; Drew, R. H.; Pickard, W. W. *Rev. Infect. Dis.* **1990**, *12*, 308−329.
(2) Hartsel, S. C.; Bolard, J. *Trends Pharmacol. Sci.* **1996**, *12*, 445−449.
(3) Ablordeppey, S. Y.; Fan, P. C.; Ablordeppey, J. H.; Mardenborough, L. *Curr. Med. Chem.* **1999**, *6*, 1151−1195.
(4) Vanden-Bossche, H.; Dromer, F.; Improvisi, I.; LozanoChiu, M.; Rex, J. H.; Sanglard, D. *Med. Mycol.* **1998**, *36*, 119−128.
(5) Andreoli, T. E. *Ann. N.Y. Acad. Sci.* **1974**, *235*, 448−468.
(6) De-Kruijff, B.; Demel, R. A. *Biochim. Biophys. Acta* **1974**, *339*, 57−70.
(7) Cohen, B. E. *Biochim. Biophys. Acta* **1986**, *857*, 117−122.
(8) Vertut-Croquin, A.; Bolard, J.; Chabbert, M.; Gary-Bobo, C. *Biochemistry* **1983**, *22*, 2939−2944.
(9) Van-Hoogevest, P.; De-Kruijff, B. *Biochim. Biophys. Acta* **1978**, *511*, 397−407.
(10) Milhaud, J.; Hartman, M. A.; Bolard, J. *Biochimie* **1989**, *71*, 49−56.
(11) Vertut-Qroquin, A.; Bolard, J.; Gary-Bobo, C. M. *Biochem. Biophys. Res. Commun.* **1984**, *125*, 360−366.
(12) Baginski, M.; Gariboldi, P.; Bruni, P.; Borowski, E. *Biophys. Chem.* **1997**, *65*, 91−100.
(13) Baginski, M.; Resat, H.; Borowski, E. *Biochim. Biophys. Acta* **2002**, *1567*, 63−78.
(14) Matsumori, N.; Sawada, Y.; Murata, M. *J. Am. Chem. Soc.* **2005**, *127*, 10667−10675.

Chart 1. Structures of AmB **1**, Ergosterol, and Cholesterol

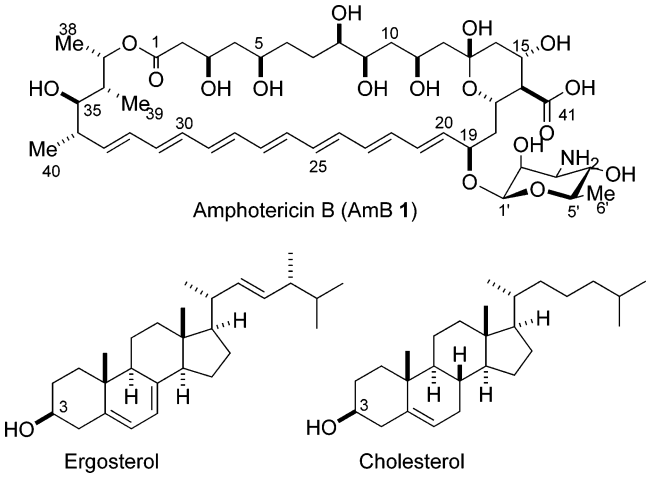

Chart 2. Structures of Intramolecular Bridged Derivatives **2**−**4** and a New One **5**

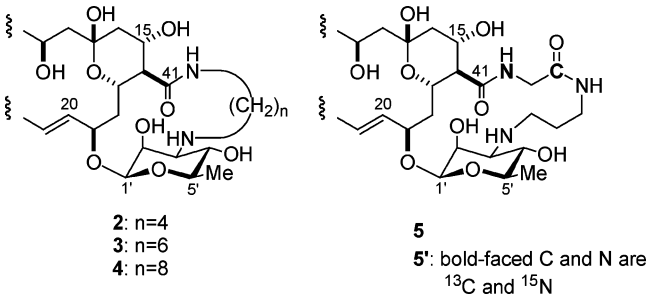

tives including **3**, however, are less active toward fungi compared with AmB, possibly because polysaccharides of the fungal cell wall, which form a strong diffusion barrier against hydrophobic molecules, reduce the penetrability through the cell wall due to the hydrophobic bridge part of the derivatives.

In this report, to gain further insight into the active conformation of AmB in the channel complex, we designed and prepared a new derivative **5**, to which a glycine-containing linker was incorporated instead of an alkyl chain to enhance the hydrophilicity of the bridge portion. We examined the conformation and activities of the derivative, which further supports our idea on the active conformation of AmB. We then investigated the dynamics of membrane-bound AmB using **5** in DMPC bilayers by solid-state NMR techniques. To facilitate the measurements, [1-^{13}C,^{15}N]glycine was introduced into the bridge. Our data implied the less mobile feature of the AmB assembly in DMPC bilayers, which suggested the formation of large aggregates in membranes.

Results and Discussion

Preparation of Intramolecular Bridged Derivative 5. In the previous report,[14] we have prepared three conformationally constrained derivatives of AmB (**2**−**4**), where their carboxyl and amino groups are intramolecularly linked with C_4, C_6, and C_8 alkyl chains, respectively. Among them, derivative **3** showed the most potent ion-channel activity and highest ergosterol selectivity. In this study we prepared a new derivative **5**, in which a glycine-containing bridge was introduced instead of alkyl chains to enhance the hydrophilicity. The chain length of derivative **5** was designed to be almost equal to that of **3**. As is the case with **3**, derivative **5** was supposed to adopt a rigid conformation due to the short bridge. The synthetic route of derivative **5** is represented in Scheme 1. Fmoc-glycine was coupled with aminopropanol to give **7**, which was then converted to aldehyde **8** by Dess−Martin oxidation. The aldehyde was coupled with the amino group of AmB by the reductive amino-alkylation reaction with use of $NaBH_3CN$. Deprotection of the Fmoc group followed by intramolecular amide formation in the presence of PyBOP as a condensation reagent afforded bridged derivative **5**. [1-^{13}C,^{15}N]glycine was used for synthesis of double-labeled **5′**.

K^+ Flux and Biological Activities. Then we assessed the K^+ flux activity of these derivatives.[15,16] The liposomes used in this assay have transmembrane gradients of pH (pH 5.5 inside and pH 7.5 outside) as well as K^+ concentration (higher on the outside). Once ion channels form, K^+ influx into the liposomes induces H^+/K^+ exchange in the presence of proton-transporter FCCP, leading to a rise in inner pH. This pH change was monitored by chemical shift changes of phosphate anions in ^{31}P NMR. Details on the spectral features of ^{31}P NMR observed in this assay are described in our recent publications.[17−22] The molar ratio of drug/lipid at which 50% of the liposomes were permeabilized was determined as EC_{50}. Table 1 lists the EC_{50} values of AmB, **3** and **5** in sterol-free, cholesterol-containing and ergosterol-containing liposomes. As is clear from the table, compound **5** shows comparable or even higher K^+-influx activity than those of AmB and **3**. In addition, the effect of cholesterol on the activity is only marginal for **5** as is the case with AmB and **3**, further supporting the idea that cholesterol is not involved in formation of the channel complex.[19,23−26] It is noteworthy that compound **5** also retains the ergosterol selectivity comparable with AmB, though less selective than **3**. Compound **5** has higher channel activity than the other two compounds in sterol-free and cholesterol-containing membranes, which partly contributes to the reduction in the ergosterol selectivity of **5** compared with that of **3**. Taken together, the hydrophilic bridge of **5**, possibly due to the formation of additional intermolecular hydrogen bonds, might stabilize the assembly even in the absence of ergosterol, thus resulting in the elevation of the channel activity without ergosterol.

We then evaluated the membrane permeabilizing activity of **5** in biological systems (Table 1). It has already been reported that the hemolytic activities (EC_{50}) of AmB and derivative **3** are 4.8 and 2.2 μM, respectively.[14] Derivative **5** also revealed potent hemolytic action at 3.0 μM. It should be noted that the antifungal activity of **5** is significantly improved in comparison

(15) Herve, M.; Cybulska, B.; Gary-Bobo, C. M. *Eur. Biophys. J.* **1985**, *12*, 121−128.
(16) Herve, M.; Debouzy, J. C.; Borowski, E.; Cybulska, B.; Gary-Bobo, C. M. *Biochim. Biophys. Acta* **1989**, *980*, 261−272.
(17) Matsumori, N.; Yamaji, N.; Matsuoka, S.; Oishi, T.; Murata, M. *J. Am. Chem. Soc.* **2002**, *124*, 4180−4181.
(18) Yamaji, N.; Matsumori, N.; Matsuoka, S.; Oishi, T.; Murata, M. *Org. Lett.* **2002**, *4*, 2087−2089.
(19) Matsuoka, S.; Murata, M. *Biochim. Biophys. Acta* **2002**, *1564*, 429−434.
(20) Matsuoka, S.; Murata, M. *Biochim. Biophys. Acta* **2003**, *1617*, 109−115.
(21) Matsuoka, S.; Matsumori, N.; Murata, M. *Org. Biomol. Chem.* **2003**, *1*, 3882−3884.
(22) Matsumori, N.; Eiraku, N.; Matsuoka, S.; Oishi, T.; Murata, M.; Aoki, T.; Ide, T. *Chem. Biol.* **2004**, *11*, 673−679.
(23) Cotero, B. V.; Rebolledo-AntUnez, S.; Ortega-Blake, I. *Biochim. Biophys. Acta* **1998**, *1375*, 43−51.
(24) Dufourc, E. J.; Smith, I. C. P.; Jarrell, H. C. *Biochim. Biophys. Acta* **1984**, *776*, 317−329.
(25) Ruckwardt, T.; Scott, A.; Scott, J.; Mikulecky, P.; Hartsel, S. C. *Biochim. Biophys. Acta* **1998**, *1372*, 283−288.
(26) Cuntinho, A.; Prieto, M. *Biophys. J.* **1995**, *69*, 2541−2557.

Scheme 1. Preparation of **5** and **5′**[a]

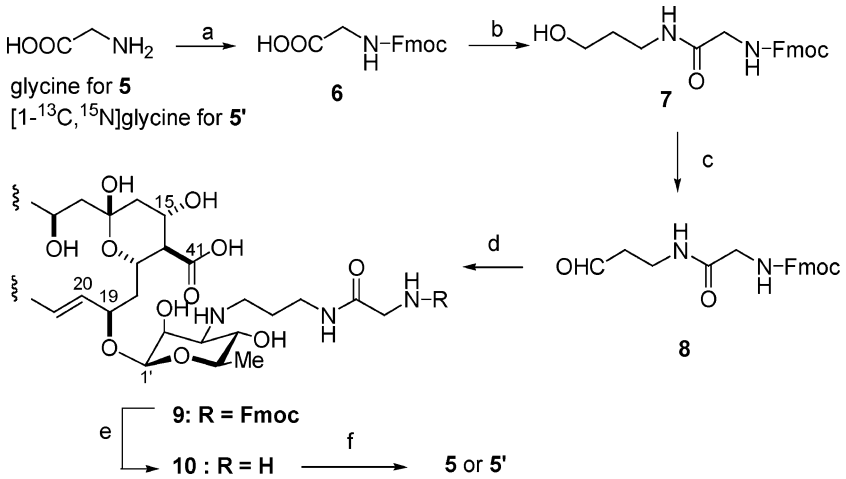

[a] Reagents: (a) Fmoc-OSu, pyridine, MeOH; (b) aminopropanol, PyBOP, HOBt, *N*-ethyldiisopropylamine, DMF; (c) Dess−Martin reagent, CH_2Cl_2; (d) AmB, $NaBH_3CN$, DMF−MeOH; (e) piperidine, DMF−MeOH; (f) PyBOP, HOBt, *N*-ethyldiisopropylamine, DMF (for product yield in each step, see Experimental Section).

Table 1. K^+ Influx Activity Using Liposomes and Biological Activities of AmB, **3**, and **5**

	K^+ influx activity EC_{50} (sample/lipid) × 10^6			hemolytic	
compound	sterol-free liposomes	cholesterol-containing liposomes	ergosterol-containing liposomes	activity[a] EC_{50}, μM	antifungal activity,[b] μg
1 (AmB)	47	43	11	4.8	5
3	60	58	5.8	2.2	20
5	30	27	9.5	3.0	10

[a] Against 1% human erythrocytes. [b] The minimal amount of samples on a paper disk that shows inhibitory zone on the culture of *Aspergillus niger*.

with **3** (Table 1). In the previous paper we postulated that hydrophilic polysaccharides of fungal cell walls form a stronger diffusion barrier against **3**, which is more hydrophobic than AmB. Accordingly, the improvement of antifungal activity in **5** may be accounted for by the enhanced hydrophilicity in the bridge portion.

Alternatively, it might be also possible to explain the improved antifungal activity of **5** by formation of water-soluble oligomers in aqueous conditions. It was reported that AmB adopts three forms in water, monomers, water-soluble oligomers, and nonsoluble aggregates, and that monomeric and water-soluble oligomeric species are biologically active.[27] To evaluate the proportion of the three forms in water, we recorded the UV and CD spectra of 5 μM AmB, **3**, and **5** in PBS buffer (see Supporting Information). Consequently, **3** mostly formed nonsoluble aggregates in water probably due to the low hydrophilicity. On the other hand, AmB and **5** formed biologically active water-soluble oligomers in buffer to a similar extent, which may be also attributed to the comparable antifungal efficacy between AmB and **5**. In both cases, the hydrophilicity must be an important index for designing new AmB derivatives in terms of amelioration of the antifungal activity.

Conformation of Intramolecular Bridged Derivative 5. We have previously determined the conformation of **3** based on distance and dihedral constraints obtained in a DMSO solution[14] and found that the orientation of the amino sugar is restricted due to the short bridge (Figure 1a). Since the ion channel property of **3** is similar yet superior to that of AmB itself, we assumed that the conformation of **3** reproduces the active conformation occurring in the channel complex of AmB. To gain further insight into the geometry of the amino-sugar in AmB, we performed conformational analysis of **5** in a similar way. The chemical shifts in the macrolide portion of **5** agreed well with those of AmB within 0.1 ppm except for the C16−C21 and the amino-sugar portion where the change in space arrangement of the sugar is likely to influence the chemical shifts (Supporting Information). Spin-coupling patterns of the macrolide rings were also similar between AmB and **5** (data not shown). These observations indicate that the macrolide conformation of **5** is virtually identical with that of AmB. Due to the possible inflexibility of the conjugated double bonds, the macrolide ring of **5** was treated as a motion-restricted part, in which a ±30° allowance from the crystal structure[28] was given to each C−C single bond upon calculation. Distance constraints for **5** were derived from 2D NOESY spectra in DMSO-d_6. The total number of interproton distances derived from the NMR data was 22. On the basis of these conformational constraints, molecular modeling calculations were performed using the Monte Carlo conformation search algorithm.[29] In comparison with **2**−**4**, derivative **5** has additional amide and glycine protons, which yielded well-resolved cross-peaks in NOESY spectra and, therefore, allowed us to extract more distance constraints around the bridged portion. Figure 1b shows superposition of 20 lowest energy conformations around the sugar portion of **5**. As in the case of **3**, derivative **5** has well converged conformers due to the constraints of the short bridge, thus implying the rigid

(27) Legrand, P.; Romero, E. A.; Cohen, B. E.; Bolard, J. *Antimicrob. Agents Chemother.* **1992**, *36*, 2518−2522.

(28) Ganis, P.; Avitabile, G.; Mechlinski, W.; Schaffner, C. P. *J. Am. Chem. Soc.* **1971**, *93*, 4560−4564.

(29) Mohamadi, F.; Richards, N. G.; Guida, W. C.; Liskamp, R.; Lipton, M.; Canfield, C.; Chang, G.; Hendrickson, T.; Still, W. C. *J. Comput. Chem.* **1990**, *11*, 440−467.

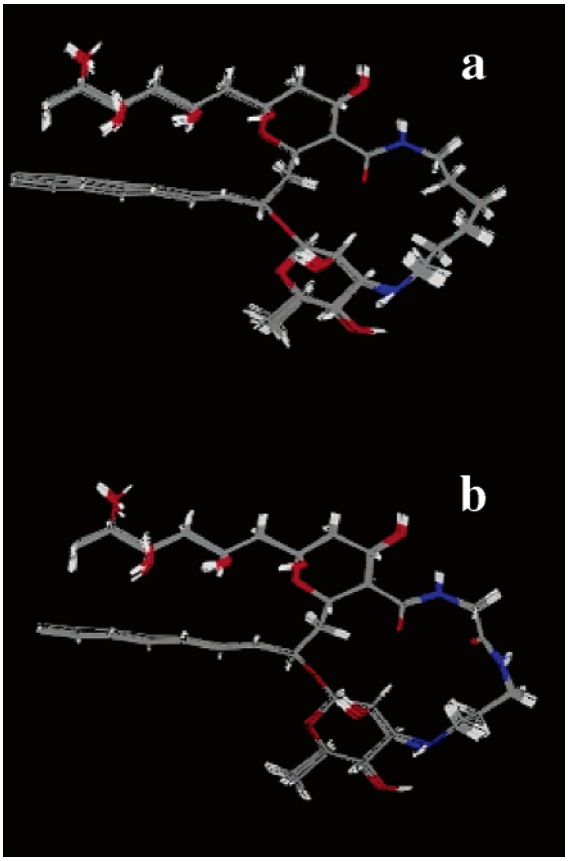

Figure 1. Ensembles of 20 lowest energy conformations for **3** (a) and **5** (b), generated by Monte Carlo algorithm restrained on the basis of distance constrains from 2D-NOESY in DMSO-d_6. Models are represented around the polar head regions of the derivatives, and 20 lowest energy conformers are superposed for a minimum rmsd. The φ (C18−C19−O−C1′) and ψ (C19−O−C1′−C2′) angles of the most stable conformer for derivative **5** are determined to be −93.2° and 149.7°, respectively, which are almost identical with those of **3** (−89.3° and 153.8°).

conformation. More importantly, the conformation of **5** agrees well with what was reported for **3**[14] (Figure 1). As described above, we have reported that the conformation of **3** probably reflects the active conformer of AmB in the channel assembly.[14] Considering that the ion-channel and biological activities of **5** are comparable to those of AmB, the rigid conformation of **5** is also thought to reproduce the active structure of AmB in the channel complex. The consistency of the conformations of **3** and **5** strongly supports this notion.

Dynamics of Intramolecular Bridged Derivative 5′ in DMPC Liposomes. With a better derivative of AmB in hand, we applied solid-state NMR techniques to obtain information on the dynamics of AmB in the membrane. The motional behavior of the derivative can provide information on the molecular assembly formed in the membrane. In this study we measured dipolar couplings and chemical shift anisotropies by solid-state NMR to investigate the molecular motion of **5** in membrane environments. For this purpose, we prepared doubly isotope-labeled **5′** using [1-^{13}C,^{15}N]glycine (Scheme 1). Dipolar couplings depend both on the internuclear distance and on molecular motion. For a fixed internuclear distance such as ^{13}C−^{15}N in **5′**, reduction in the coupling strength from its rigid lattice value is caused only by motional averaging. The scaling factor between the measured coupling constant and the rigid-limit value is the order parameter S, which provides information about the

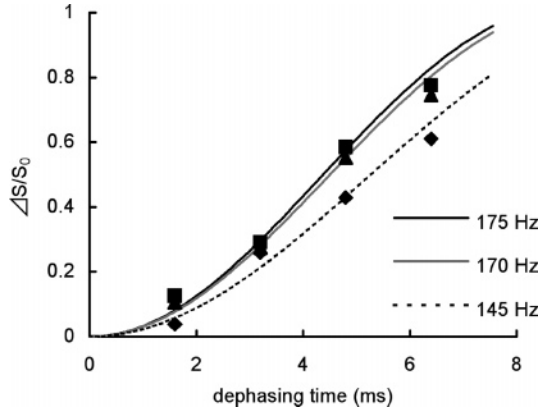

Figure 2. Experimental ^{13}C−^{15}N REDOR dephasing values ($\Delta S/S_0$) of **5′** in powder form (■), in membranes of ergosterol-containing DMPC (▲), and sterol-free DMPC (◆). Dark solid, light solid, and dotted lines are the best-fit curves for the square points, triangles, and diamonds, respectively.

amplitude of motion and, in favorable cases, the orientation of the internuclear vector relative to the motional axis. Accordingly, we measured ^{13}C−^{15}N dipolar couplings of **5′** in DMPC membranes using REDOR experiments.[29] Figure 2 shows the ^{13}C−^{15}N REDOR dephasings of **5′** in the powder form and in DMPC membranes in the presence and absence of ergosterol (**5′**/ergosterol/DMPC 1:1:9 or 1:0:10). ^{13}C−^{15}N dipolar coupling values obtained from the best-fit dephasing curves are also depicted in Figure 2. The rigid-limit C−N dipolar coupling of **5′** is calculated to be 198 Hz on the basis of the C−N internuclear distance 2.49 Å. Bond vibration and imperfection of π pulses in REDOR measurements may scale down the dipolar coupling to 175 Hz even in the powder form.[31,32] Surprisingly, the dipolar coupling of **5′** in the ergosterol-containing DMPC membrane (170 Hz) is almost the same as that in the powder form, while that in the sterol-free DMPC membrane is significantly attenuated to be 145 Hz. These dipolar couplings indicate that **5′** is almost immobilized in the ergosterol-containing DMPC membrane, while a small amount of mobility remains in the sterol-free DMPC membrane. The attenuated dipolar coupling of **5′** in the sterol-free DMPC membrane can be interpreted in two ways. One possibility is that both mobile and immobile molecules coexist in the membrane, and the mobile molecules contribute to the reduction of the dipolar coupling. The other possibility is that all of **5′** molecules undergo whole-body fast rotation in the sterol-free DMPC membrane. If the rotation is uniaxial, the order parameter is represented by $(1 - 3\cos^2\theta)/2$, which yields the θ angle of ca. 20° between the rotation axis and the C−N direction.

Further information of the dynamics of **5′** was obtained from ^{13}C chemical shift anisotropies. Changes in chemical shift tensors also signify molecular motion. Figure 3 illustrates the ^{13}C cross-polarization spectra of **5′** in the powder form and in DMPC membranes in the presence and absence of ergosterol. The spectra in DMPC membranes were acquired at slow MAS of 1 kHz to generate spinning sidebands for sensitivity enhancement. As is clear from Figure 3, the powder patterns expressed by the sidebands are almost consistent in all spectra, indicating identical chemical shift tensors even in membranes. This result

(30) Gullion, T.; Schaefer, J. *J. Magn. Reson.* **1989**, *81*, 196−200.
(31) Saito, H.; Tuzi, S.; Naito, A. *Annu. Rep. NMR Spectrosc.* **1998**, *36*, 79−121.
(32) Naito, A.; Saito, H. *Encycl. Nucl. Magn. Reson.* **2002**, *9*, 283−291.

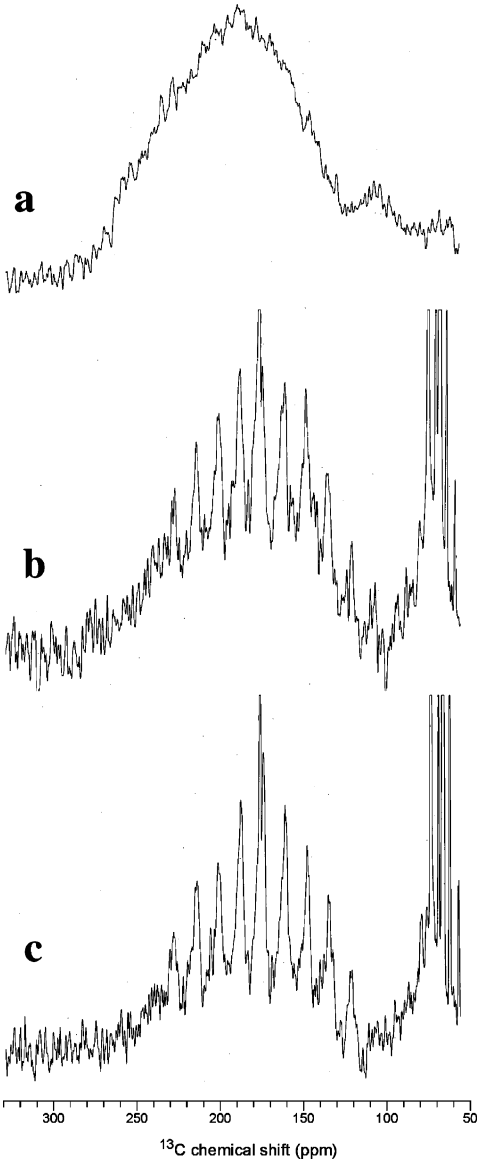

Figure 3. ^{13}C powder patterns of **5′** in powder form (a), ergosterol−DMPC (b), and sterol-free DMPC (c). The molar ratios of **5′**/ergosterol/DMPC are 1:1:9 for ergosterol-containing liposome and 1:0:10 for sterol-free one. Spectra b and c obtained in membranes were recorded under MAS at 1 kHz. Sharp signals at 173 ppm in spectra b and c are due to carbonyl carbon atoms of esters in DMPC.

rules out the possibility of uniaxial fast molecular rotation of **5′** in the sterol-free DMPC membrane and further supports the immobility of **5′** in the ergosterol−DMPC membrane.

However, whether both mobile and immobile molecules are present in the sterol-free membrane was not clear from Figure 3. Hence, to gain further evidence on the presence of mobile molecules in sterol-free DMPC membrane, we performed dipolar-decoupling (DD)-MAS experiments.[31] In DD-MAS experiments, as opposed to the cross-polarization method, molecules with high mobility yield stronger signals. The broader ^{13}C signal at 171 ppm of **5′** in sterol-free DMPC was significantly stronger that that in ergosterol-containing DMPC (Figure 4), thus supporting the presence of a larger amount of movable molecules in sterol-free DMPC bilayers. The signal at 171 ppm in the ergosterol-containing membrane is thought to be mostly due to immobilized molecules because the powder form of **5′** also gave the signal in the DD-MAS experiment (data

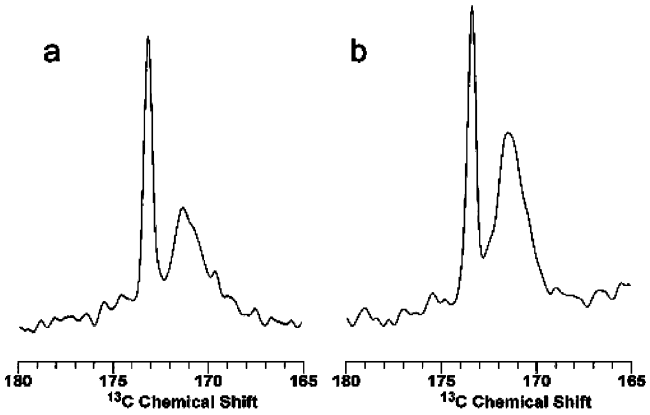

Figure 4. DD-MAS ^{13}C spectra of **5′** in ergosterol-containing (a) and sterol-free (b) DMPC bilayers. The signals at 171 ppm are due to the labeled glycine moiety of **5′**, while those at 173 ppm are from the ester groups of DMPC bilayers, which are used for internal standards to compare the ^{13}C signal intensity of **5′**.

not shown). The broad signals of **5′** further reveal that monomeric or oligomeric forms, which were observed in the aqueous phase as described earlier, hardly occurred under these NMR conditions.

The above results totally suggested that **5′** is mostly immobilized in ergosterol-containing DMPC membranes while a considerable amount of movable molecules coexist in the sterol-free DMPC membrane. Some membrane peptides are known to form aggregates in the membrane and consequently show low mobility.[33] Therefore, the current results can also be accounted for by the aggregate formation of **5′** in DMPC membranes. Recently we have shown that the AmB molecule can span the DMPC bilayer with a single molecular length by measuring dipolar interactions between ^{13}C labeled AmB and ^{31}P of a phospholipid using the same membrane preparation.[34] The relatively large $^{13}C-^{31}P$ dipolar interactions also indicated the formation of a tight complex of AmBs and phospholipids. Since the membrane permeabilizing activities of **5** are quite similar to those of AmB, the previous results obtained for AmB would hold true for derivative **5**. Taken together, it can be assumed that derivative **5** and boundary DMPC molecules form an immobilized complex in the bilayer under the present conditions. This notion is supported by earlier ^{2}H NMR studies which also suggest that DMPC is immobilized in the presence of AmB.[35]

Here it should be emphasized that **5′** is immobilized on a time scale of 5 ms or longer, which corresponds to the inverse of the C−N dipolar interaction of ca. 200 Hz. Although chemical shift anisotropy and quadrupolar coupling, which are large interactions over 10^4 Hz, are frequently used for motional study of membrane peptides in lipid bilayers, measurements of these interactions can only provide information about the mobility of membrane-bound molecules on time scales shorter than the inverse of the interactions (μs orders). Accordingly, the advantage in weak dipolar couplings used in this study is the detection capability of the immobilization on millisecond scales.

Based on the rotational correlation time slower than 5 ms, we can roughly estimate the size of the aggregate of **5′** in the

(33) Buffy, J. J.; Waring, A. J.; Lehrer, R. I.; Hong M. *Biochemistry* **2003**, *42*, 13725−13734.
(34) Matsuoka, S.; Ikeuchi, H.; Matsumori, N.; Murata, M. *Biochemistry* **2005**, *44*, 704−710.

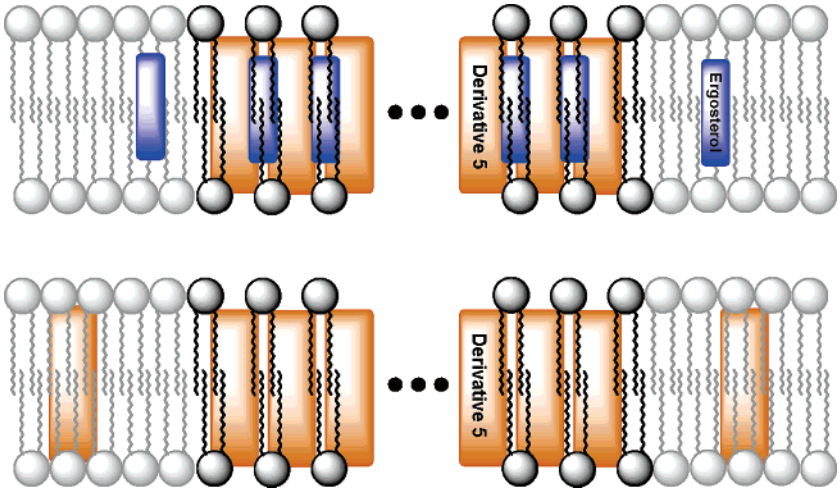

Figure 5. Models of aggregate formation of AmB derivative **5** in DMPC bilayers in the presence (top) and absence (bottom) of ergosterol. In the presence of ergosterol, **5** aggregates with DMPC and possibly with ergosterol to form immobilized domains larger than 20 nm in diameter. Immobilized aggregates of **5** are also formed even in the absence of ergosterol, although some fraction of **5** probably remains mobilized.

membrane since the rotational diffusion rate is inversely proportional to the aggregate size. According to the two-dimensional hydrodynamic model,[36] a cylindrical particle with a radius of a and thickness of h has a rotational diffusion coefficient D_R as follows:

$$D_R = \frac{1}{\tau_R} = \frac{k_B T}{4\pi\eta\, a^2 h}$$

where τ_R is the rotational correlation time, η is the viscosity of the lipid bilayer, k_B is the Boltzmann constant, and T is the absolute temperature. Since we have shown that the AmB molecule traverses the DMPC bilayer with a single molecular length,[34] which should be the case with **5**, h can be estimated as ca. 40 Å, corresponding to the thickness of the DMPC bilayer. A conservative upper-limit estimate of the membrane viscosity is 10 P.[37] Using these values, a motional correlation time τ_R longer than 5 ms yields an aggregate radius larger than 20 nm. The pore size of the AmB ion channel is estimated as 0.6−0.8 nm,[38−41] and the external diameter is reported to be around 1.7 nm.[41] Therefore, it is unlikely that the radius of a single ion channel complex exceeds 20 nm, even if boundary phospholipid molecules are involved in the complex. Rather it is more likely that ion channel complexes gather and form immobilized domainlike aggregates with a radius larger than 20 nm. This speculation is supported by the recent results of AFM observations of large AmB aggregates.[42]

Figure 5 summarizes our current model of aggregation of **5** in DMPC membranes. In the ergosterol−DMPC membrane, **5** together with DMPC and ergosterol forms immobilized aggregates, which possess a diameter larger than 20 nm and are phase-separated from liquid-crystalline bilayers. On the other hand, in the sterol-free DMPC membrane, although a large part of the AmB molecules form immobilized aggregates with phospholipids, mobile molecules, which are possibly sequestered from the aggregates, are also present to a considerable extent. In the aggregates, **5** is thought to traverse the membrane with a single molecular length, as previously shown in AmB by $^{13}C-^{31}P$ REDOR experiments.[34] The higher aggregate formation in the presence of ergosterol may be ascribable to the action of ergosterol as a glue to stick the AmB derivatives, which further shifts the equilibrium from monomer (or small oligomer) to aggregates. Considering that the biological and ion-permeable activities are almost equivalent between AmB and **5**, it may be possible to extrapolate this model to AmB itself.

Hing et al. have reported that the methyl-d_3 amide derivative of AmB undergoes fast rotation in the DPPC bilayer,[43] which is in contrast to the present data. This is probably due to the different drug/lipid ratio; they adopted a lower ratio (ca 1 mol %) compared with the current study (10 mol %). Earlier circular dichroism (CD) studies by Perkins et al. also suggested that AmB at less than 3 mol % of DMPC−DMPG was largely monomeric.[44] To observe the molecular assembly of AmB by NMR, we are obliged to use higher drug/lipid ratios although the drug exerts its effects at much lower doses, where a small fraction of AmB molecules are thought to form ion channel aggregates. Our preliminary results of solid-state NMR experiments using deuterated AmB suggest that immobilized AmB in large aggregates, which are predominant at 10 mol % AmB in DMPC, partly exists even at 1 mol % AmB in DMPC (to be published in due course). Since the complex formation is thought to be necessary for the ion-channel activity of AmB, the motionally restricted aggregates formed by bridged derivative **5** may be reasonably related to the molecular assembly of AmB acting as an ion channel. In that context, these aggregates would provide relevant information on the ion channel structure of AmB as wall as intermolecular interactions in the channel complex. Further structural studies of the aggregates using solid-state NMR are currently underway.

(35) Dufourc, E. J.; Smith, I. C. P.; Jarrell, H. C. *Biochim. Biophys. Acta* **1984**, *778*, 435−442.
(36) Saffman, P. G.; Delbruck, M. *Proc. Natl. Acad. Sci. U.S.A.* **1975**, *72*, 3111−3113.
(37) Tamm, L. K. *Biochim. Biophys. Acta* **1991**, *1071*, 123−148.
(38) Scherrer, R.; Gerhardt, P. *J. Bacteriol.* **1971**, *107*, 718−735.
(39) Katsu, T. *Biol. Pharm. Bull.* **1999**, *22*, 978−980.
(40) Houdai, T.; Matsuoka, S.; Matsumori, N.; Murata, M. *Biochim. Biophys. Acta* **2004**, *1667*, 91−100.
(41) Gruszecki, W. I.; Gagos, M.; Kernen, P. *FEBS Lett.* **2002**, *524*, 92−96.
(42) Milhaud, J.; Ponsinet, V.; Takahashi, M.; Mchels, B. *Biochim. Biophys. Acta* **2002**, *1558*, 95−108.
(43) Hing, A. W.; Schaefer, J.; Kobayashi, G. S. *Biochim. Biophys. Acta* **2000**, *1463*, 323−332.
(44) Perkins, W. R.; Minchey, S. R.; Boni, L. T.; Swenson, C. E.; Popescu, M. C.; Pasternack, R. F.; Janoff, A. S. *Biochim. Biophys. Acta* **1992**, *1107*, 271−282.

Conclusion

We have designed and prepared a new intramolecular bridged derivative **5** and showed that **5** excellently retained membrane permeabilizing activity and selective toxicity characteristic of AmB. The conformation of **5**, restricted with a short-chain bridge, was similar to that of derivative **3** which has the highest ergosterol selectivity among homologues with different lengths of bridges. This indicates that the orientation of aminosugars in **3** and **5** is critical to the activity of AmB, thus further confirming the idea that the conformation of the bridged derivatives reflects the active structure of AmB in the channel complex.

Isotope-labeled derivative **5′** was then subjected to solid-state NMR measurements in DMPC membrane preparations, which demonstrated that **5** forms immobilized aggregates in the membranes. It was also observed that the aggregate formation is promoted in the presence of ergosterol, which might be related to the higher activity of AmB in ergosterol-containing membranes. Because derivative **5** has biological activity and ion-channel properties similar to those of AmB, it is assumed that motional properties of **5** somewhat reflect the behaviors of AmB upon ion-channel formation.

Experimental Section

Materials and Methods. Amphotericin B (AmB), egg phosphatidylcholine, amino-alcohols, cholesterol, and ergosterol were from Nakarai Tesque. 1,2-Dimyristoyl-*sn*-glycero-3-phosphocholine (DMPC) was purchased from Avanti Polar Lipid Inc. (Alabaster, AL). [1-^{13}C,^{15}N]-glycine was from Cambridge Isotope Laboratory (Cambridge, MA). Deuterated solvents were purchased from Merck. All other chemicals were obtained from standard venders and used without further purification. NMR spectra were recorded on a JEOL GSX-500 spectrometer. ESI-MS spectra were measured on an LCQ-deca (Thermo Finnigan). HPLC was performed on a Shimadzu LC-10ADvp with an SPD-M10Avp photodiode array detector. Thin-layer chromatography (TLC) was performed on a glass plate precoated with silica gel (E. Merck Kieselgel 60 F254). Column chromatography was performed with silica gel 60 (E. Merck, particle size 0.063−0.200 mm, 60−230 mesh).

***N*-(9-Fluorenylmethoxycarbonyl)-glycyl-3-aminopropanol (6).** Fmoc-glycine was prepared with a standard method. To a stirred solution of Fmoc-glycine (120 mg, 0.30 mmol) and 3-aminopropanol (46μL, 40 μmol, 0.60 mmol) in DMF (12 mL) were added diisopropylethylamine (138 μL, 0.80 mmol), 1-hydroxybenzotriazole (74 mg, 0.48 mmol), and PyBOP (208 mg, 0.40 mmol) sequentially. After being stirred at 23 °C for 16 h, the mixture was diluted with water (100 mL) and extracted with $CHCl_3$. The organic layer was dried over $MgSO_4$, concentrated, and purified by column chromatography on SiO_2 with $CHCl_3$−MeOH to give **6** as a white amorphous powder (89 mg, 63%). R_f 0.41 ($CHCl_3$−MeOH = 5:1). ^{1}H NMR (500 MHz, $CDCl_3$) δ 7.74 (d, 2H, J = 7.0 Hz), 7.57 (d, 2H, J = 7.0 Hz), 7.39 (t, 2H, J = 7.5 Hz), 7.30 (t, 2H, J = 7.5 Hz), 6.43 (brs, 1H), 5.38 (brs, 1H), 4.44 (d, 2H, J = 7.0 Hz), 4.20 (t, 1H, J = 7.0 Hz), 3.83 (d, 2H), 3.62 (t, 2H), 3.42 (m, 2H), 1.67 (m, 2H).

***N*-(9-Fluorenylmethoxycarbonyl)-glycyl-3-aminopropanal (7).** To a CH_2Cl_2 solution (1 mL) of **6** (150 mg, 0.48 mmol) was added Dess−Martin reagent (220 mg, 0.52 mmol) at 23 °C. After being stirred for 3 h, the solution was quenched with 10 mL of saturated $Na_2S_2O_3$ solution and extracted with $CHCl_3$. The organic layer was dried over $MgSO_4$ and concentrated in vacuo, yielding crude **7** as a white amorphous powder (69 mg, 72%). R_f 0.41 ($CHCl_3$−MeOH = 5:1). ^{1}H NMR (500 MHz, $CDCl_3$) δ 9.77 (s, 1H), 7.74 (d, 2H, J = 7.5 Hz), 7.57 (d, 2H, J = 7.5 Hz), 7.38 (t, 2H, J = 7.5 Hz), 7.30 (t, 2H, J = 7.5 Hz), 6.39 (brs, 1H), 5.38 (brs, 1H), 4.41 (d, 2H, J = 7.0 Hz), 4.20 (t, 1H, J = 7.0 Hz), 3.80 (d, 2H), 3.54 (m, 2H), 2.73 (m, 2H).

***N*-{*N*-(9-Fluorenylmethoxycarbonyl)-glycyl-3-aminopropyl}-AmB (8).** A solution of **7** (13 mg, 36 μmol) and AmB (50 mg, 54 μmol) in DMF−MeOH (4:3, 7 mL) was stirred for 3 h, and then $NaBH_3$-CN (14 mg, 216 μmol) was added to the solution. After being stirred overnight, the solution was poured into diethyl ether (100 mL) to form a yellow precipitate, which was filtered over Celite and washed with diethyl ether. The precipitate and the Celite were extracted with $CHCl_3$−MeOH−H_2O 10:6:1 and purified by column chromatography on SiO_2 with the same solvent system to afford **8** (19 mg, 43%) as a yellow solid. R_f 0.63 ($CHCl_3$−MeOH−H_2O = 10:6:1. ESI-MS m/z 1260.4 $(M + H)^+$.

Preparation of Derivatives 5 and 5′. To a solution of **8** (19 mg, 15 μmol) in DMF−MeOH (1:1, 4 mL) was added piperidine (500 μL, 5 mmol). After the solution stirred for 30 min, diethyl ether was added to form a yellow precipitate. The precipitate was filtered over Celite and washed with diethyl ether. The product was extracted with $CHCl_3$−MeOH−H_2O to give crude **9** (18 mg), which was used for the next reaction without further purification because of instability. To a solution of crude **9** (18 mg) in DMF (10 mL) were added diisopropylethylamine (6 μL, 35 μmol), 1-hydroxybenzotriazole (3.3 mg, 21 μmol), and PyBOP (8.8 mg, 17 mmol) sequentially. After the mixture stirred for 20 h, it was poured into diethyl ether to form precipitates. The precipitate was filtered over Celite, washed with diethyl ether, and extracted with $CHCl_3$−MeOH−H_2O. The extract was purified by HPLC to afford **2** (1.7 mg, 11% for two steps). HPLC conditions: column, COSMOSIL 5C_{18}-AR-II Φ 4.6 mm × 150 mm; flow rate, 0.5 mL/min; mobile phase, MeOH−5 mM ammonium acetate (pH 5.3) changing linearly from 70:30 to 100:0 for 30 min; retention time, 20.0 min. ESI-MS m/z 1020.5 $(M + H)^+$. ^{1}H NMR (500 MHz, DMSO-d_6), see Supporting Information. **5′** was prepared in the same way as **5** by using [1-^{13}C,^{15}N]glycine as a starting material.

Liquid NMR Measurements. The antibiotic solutions were prepared under dry argon in DMSO-d_6 at 5 mM concentration. All liquid NMR spectra were recorded at 25 °C on a JEOL GSX500 spectrometer (^{1}H 500 MHz). Spectra were processed using Alice2 V.4.1 (JEOL DATUM) software. Homonuclear two-dimensional spectra COSY, TOCSY (HOHAHA), and NOESY were recorded with a 1.5 s recovery delay in the phase-sensitive mode using the States method as data matrices of 512 ($F1$) × 1024 ($F2$) complex data points. Mixing times of 80 ms for TOCSY and 300 ms for NOESY spectra were used. The spectral width in both dimensions was 5000 Hz. The data were apodized with shifted square sine-bell window functions in both $F1$ and $F2$ dimensions after zero-filling in the $F2$ dimension to obtain a final matrix of 512 ($F1$) × 2048 ($F2$) real data points. Chemical shifts were referenced to the solvent chemical shift (DMSO-d_5(^{1}H), 2.49 ppm.).

Conformation Analysis of 5. All the interproton-distance restraints between non-J-coupled protons are derived from the two-dimensional homonuclear NOESY experiments. Interproton restraints were classified into three categories. Upper bounds were fixed at 2.8, 3.4, and 4.0 Å for strong, medium, and weak correlations, respectively. A lower bound was fixed at 1.8 Å, which corresponds to the sum of the hydrogen van der Waals radii. Pseudo atom corrections of the upper bounds were applied for distance restraints involving the unresolved methylene and methyl protons (+1 Å). For stereospecifically assigned diastereotopic methylene protons, the interproton distances were applied to each proton according to the NOE peak intensities. When possible, H−C−C−H dihedral angles were restrained to dihedral domains according to the different $^3J_{HH}$ coupling constants measured using Karplus dihedral relations with a ±30° allowance. Conformation was calculated using the MacroModel software version 8.5[29] installed on RedHat Linux 8 OS. Initial atomic coordinates and structure files were generated step-by-step from the crystal data of *N*-iodoacetyl AmB.[28] The macrolide ring was treated as a semirigid group, in which a ±30° allowance from the crystal structure[28] was given to each C−C single bond upon calculation. The sampling of the conformational space was performed

following a Monte Carlo Multiple Minimum method.[45] The MMFF force field[46] implemented in the MacroModel was used. The nonbonded van der Waals interactions were represented by a simple repulsive quadratic term. The experimental distance restraints were represented as a soft asymptotic potential, and electrostatic interactions were ignored. 5000 steps of MCMM were carried out.

K^+ Flux Assays Using ^{31}P NMR. Egg phosphatidylcholine (52.0 μmol) or egg phosphatidylcholine-sterol (46.8 and 7.2 μmol) was dissolved in $CHCl_3$ (2 mL), and the mixture was evaporated to a thin film in a round-bottom flask. After dried in vacuo for over 8 h, pH 7.5 buffer (0.726 mL) containing KH_2PO_4 (0.4 mM) and EDTA (1 mM) was added to the flask. The lipid mixture was suspended in the buffer by vortexing and sonication. The resultant suspension was frozen at −20 °C and thawed at 50 °C 3 times. The liposome solution thus obtained was passed repeatedly through a membrane filter (pore size, 0.2 μm, 19 times) with a Liposofast apparatus (AVESTIN) and then diluted with K_2SO_4 (0.4 M, 3.63 mL) to give a 12 mM LUV solution. The LUV suspension was adjusted to pH 7.5 with 10 M KOH. A 750 μL aliquot of the LUV suspension was transferred to a 1.5 mL Eppendorf tube and mixed with 2 μL of 10 mM carbonyl cyanide-*p*-trifluoromethoxyphenyl hydrazone (FCCP) ethanol solution and 2 μL of a DMSO solution of drugs. After incubation for 6 h at room temperature, a 550 μL portion was transferred to a 5-mm NMR glass tube and mixed with 4.4 μL of 100 mM $MnCl_2$. ^{31}P NMR spectra were recorded at 23 °C on a JEOL GSX-500 spectrometer (^{31}P at 202.35 MHz) with ^1H-broad band decoupling. The assay was generally repeated more than 3 times for each sample with good reproducibility. The activity was evaluated by the decrease in peak area at δ 1.2. From the concentration−activity relationship, EC_{50} values were determined.

Biological Activities. For hemolytic assays, freshly collected human blood was centrifuged for 5 min at 1000 *g*, and separated erythrocytes were washed twice by suspending in PBS buffer (pH 7.4). Packed erythrocytes were then resuspended with PBS to a 100-fold volume of the original blood. Gradually diluted drug solutions (DMSO solution, 2 μL) were added to the erythrocyte suspensions (198 μL), and the suspensions were incubated with gentle shaking at 37 °C. After 18 h, the suspensions were spun and the absorbance of the supernatant was determined at 490 nm by a microplate reader (Molecular Devices). For a positive control, water was used instead of a PBS buffer. As a negative control, 2 μL of DMSO were added instead of the sample solution. From dose−response curves, the dosage that led to 50% hemolysis (EC_{50}) was determined.

For antifungal assays, *Aspergillus niger* was cultured in a GP liquid medium (2% glucose, 0.2% yeast extract, 0.5% polypeptone, 0.05% $MgSO_4$, and 0.1% KH_2PO_4) at 25 °C for 2 days. An aliquot of the broth was then spread onto a GP agar plate. The drugs dissolved in DMSO were spotted on paper disks 8 mm in diameter. As a control, a disk containing only DMSO was also prepared. These paper disks were then placed on an agar plate containing *A. niger* mycelia. After cultivating at 25 °C for 2 days, the diameter of the inhibitory zone on each paper disk was measured.

Solid-State NMR Measurements. For membrane preparation, a combination of 2.6 mg of **5′** and 16.7 mg of DMPC (molar ratio 1:10) or that of 2.6 mg of **5′**, 15.1 mg DMPC, and 1.0 mg of ergosterol (1:9:1) was mixed in $CHCl_3$−MeOH (6:1), and the solvent was removed in vacuo for 8 h. The dried membrane was hydrated with 19.3 μL of 10 mM HEPES buffer (pH 7.0) under Ar and then diluted with 1 mL of H_2O. After a few minutes of sonication, the membrane was freeze−thawed 3 times and vortexed to make multilamellar vesicles. The suspension was lyophilized, rehydrated with 19.3 μL of D_2O, and transferred into a glass insert (Wilmad) for a ϕ 5-mm MAS rotor, which was sealed with epoxy glue. Then the glass insert was set to the ϕ 5-mm MAS rotor. For the powder sample of **5′**, 5 mg of **5′** was mixed with Celite and packed into the ϕ 5-mm MAS rotor. Solid-state NMR experiments were carried out on a CMX300 (Varian/Chemagnetics) spectrometer operating at a resonance frequency of 299.494 MHz for ^1H, 75.320 MHz for ^{13}C, and 30.351 MHz for ^{15}N. Cross-polarization spectra of ^{13}C were obtained under no spinning for the powder sample and 1 kHz MAS for membrane samples. $^{13}C\{^{15}N\}$ REDOR spectra[30] were acquired with the MAS frequency of 5000 ± 2 Hz. DD-MAS spectra were obtained with single-pulse excitation of ^{13}C under 5 kHz MAS. In all measurements, the rotor temperature was kept at 30 ± 1 °C by a temperature controller, and the spectral width was 30 kHz. Typically a 90° pulse width for ^1H was 2.5 μs, and 180° pulse widths for ^{13}C and ^{15}N were 7 μs and 14 μs, respectively. The contact time for cross polarization transfer was set to be 2 ms. Spectra were acquired with a recycle delay of 5 s and a ^1H decoupling field strength of 75 kHz. REDOR spectra were measured at dephasing times of 1.6, 3.2, 4.8, and 6.4 ms, using xy-8 phase cycling for ^{15}N irradiations.[47]

Acknowledgment. We are grateful to Prof. Tohru Oishi and Dr. Shigeru Matsuoka in our laboratory for invaluable discussions. This work was supported by Grants-In-Aids for Scientific Research A) (No. 15201048) and for Young Scientists (B) (No. 14780458) from MEXT, Japan.

Supporting Information Available: NMR spectra and NOE correlations for **5**; UV and CD spectra of **1**, **3**, and **5** in PBS buffer. This material is available free of charge via the Internet at http://pubs.acs.org.

JA063433W

(45) Kolossvary, I.; Guida, W. C. *J. Comput. Chem.* **1999**, *20*, 1671−1684.
(46) Halgren, T. A. *J. Comput. Chem.* **1999**, *20*, 730−748.
(47) Gullion, T.; Baker, D. B.; Conradi, M. S. *J. Magn. Reson.* **1990**, *89*, 479−484.